research articles Journal of proteome research

Integrative Proteomic and Cytological Analysis of the Effects of Extracellular Ca^{2+} Influx on *Pinus bungeana* Pollen Tube Development

Xiaoqin Wu,[†,‡,#] Tong Chen,[†,§,#] Maozhong Zheng,[†,§] Yanmei Chen,[†] Nianjun Teng,[†,§] Jozef Šamaj,[||,⊥] František Baluška,[||,¶‖] and Jinxing Lin*[,†]

Key Laboratory of Photosynthesis and Molecular Environment Physiology, Institute of Botany, Chinese Academy of Sciences, 100093 Beijing, China, Systematic and Evolutionary Botany, South China Botanical Garden, Chinese Academy of Sciences, Guangzhou 510650, China, Graduate School of Chinese Academy of Sciences, Beijing 100049, China, Department of Plant Cell Biology, Institute of Cellular and Molecular Botany, Rheinische Friedrich-Wilhelms-University Bonn, D-53115 Bonn, Germany, Institute of Plant Genetics and Biotechnology, Slovak Academy of Sciences, SK-95007 Nitra, Slovak Republic, and Institute of Botany, Slovak Academy of Sciences, SK-84223 Bratislava, Slovak Republic

Received April 1, 2008

Ca^{2+} is an essential ion in the control of pollen germination and tube growth. However, the control of pollen tube development by Ca^{2+} signaling and its interactions with cytoskeletal components, energy-providing pathways, and cell-expansion machinery remain elusive. Here, we used nifedipine (Nif) to study Ca^{2+} functions in differential protein expression and other cellular processes in *Pinus bungeana* pollen tube growth. Proteomics analysis indicated that 50 proteins showed differential expression with varying doses of Nif. Thirty-four of these were homologous to previously reported proteins and were classified into different functional categories closely related to tip-growth machinery. Blocking the L-type Ca^{2+} channel with Nif in the pollen tube membrane induced several early alterations within a short time, including a reduction of extracellular Ca^{2+} influx and a subsequently dramatic decrease in cytosolic free Ca^{2+} concentration ($[Ca^{2+}]_c$), concomitant with ultrastructural abnormalities and changes in the abundance of proteins involved in energy production and signaling. Secondary alterations included actin filament depolymerization, disrupted patterns of endocytosis/exocytosis, and cell wall remodeling, along with changes in the proteins involved in these processes. These results suggested that extracellular Ca^{2+} influx was necessary for the maintenance of the typical tip-focused $[Ca^{2+}]_c$ gradient in the *P. bungeana* pollen tube, and that reduced adenosine triphosphate production (ATP), depolymerization of the cytoskeleton, and abnormal endocytosis/exocytosis, together with enhanced rigidity of cell walls, were responsible for the growth arrest observed in pollen tubes treated with Nif.

Keywords: calcium • nifedipine • *Pinus bungeana* • proteomics • pollen tube

Introduction

Pollen tubes represent a robust model system for investigating tip growth. Basic information regarding angiosperm pollen tube biology has long been known.[1,2] It is only recently, however, that major new insights regarding intracellular signal cascades, the cytoskeleton, and endo/exocytosis in angiosperm pollen tubes have come to light.[3−5] Pollen tube growth in conifers differs from that in angiosperms in several parameters, such as growth rate, cytoskeleton organization, and endo/exocytosis.[6−9] Therefore, it is unlikely that the mechanism of polarized growth is the same in angiosperm and gymnosperm species. Previous research has created a foundation for a better understanding of the biochemical processes of gymnosperm pollen tube development.[10−12] Nevertheless, gymnosperm pollen tube growth is still far from fully understood, particularly with regard to the role of cytosolic Ca^{2+} dynamics which differ from those in angiosperms.[12]

The inhibitor nifedipine (Nif), or 1, 4-dihydro-2, 6-dimethyl-4-(2-nitrophenyl)-3, 5 pyridine-dicarboxylic acid dimethyl ester, has been used successfully to treat various types of angina and hypertension.[13] There is increasing evidence of a striking effect of Nif on extracellular Ca^{2+} influx by blocking voltage-gated L-type Ca^{2+} channels. This makes the inhibitor useful for elucidating the biological processes connected with Ca^{2+} influx

* To whom correspondence should be addressed. Prof. Jinxing Lin, Key Laboratory of Photosynthesis and Molecular Physiology, Institute of Botany, Chinese Academy of Sciences, Beijing 100093, China. Tel: 0086-10-62836211. Fax: 0086-10-62590833. E-mail: linjx@ibcas.ac.cn.
† Institute of Botany, Chinese Academy of Sciences.
‡ South China Botanical Garden, Chinese Academy of Sciences.
§ Graduate School of Chinese Academy of Sciences.
# These authors contributed equally to this work.
|| Rheinische Friedrich-Wilhelms-University Bonn.
⊥ Institute of Plant Genetics and Biotechnology, Slovak Academy of Sciences.
¶‖ Institute of Botany, Slovak Academy of Sciences.

10.1021/pr800241u CCC: $40.75

Published on Web 08/21/2008

and $[Ca^{2+}]_c$ gradient.[14−16] Using a laser scanning confocal microscope (LSCM) and patch-clamp, Shang et al. reported that a hyperpolarization-activated Ca^{2+}-permeable channel on pollen protoplast membrane could be suppressed by Nif and $[Ca^{2+}]_c$ subsequently decreased.[17] Moreover, studies on lily pollen tubes established that Nif treatment altered the tip-focused $[Ca^{2+}]_c$ gradient markedly accompanied by irregular tube growth, resulting in growth arrest.[18,19] The improved Ca^{2+} detection techniques including relevant fluorescence imaging and ion-selective vibrating electrode enabled the detection of extracellular Ca^{2+} influx and the $[Ca^{2+}]_c$ gradient in growing pollen tubes.[2,20] These results demonstrated that a tip-focused $[Ca^{2+}]_c$ gradient regulated the direction of pollen tube growth, endo/exocytosis in the pollen tube apex, and the organization of the actin cytoskeleton.[19,21−23] However, these studies were largely focused on angiosperm pollen tubes. Much less is known about the precise roles of the tip-focused $[Ca^{2+}]_c$ in gymnosperm pollen tube growth. Moreover, the mechanisms that maintain the $[Ca^{2+}]_c$ gradient remain unclear.

Proteomics is an emerging molecular tool for identifying proteins involved in specific biological responses.[10,24] Recent studies have indicated that the pollen-specific gene-expression pattern, which is required for normal pollen development, can be altered in response to treatment with inhibitors.[11,25] Proteomics would permit the exploration of pollen tube growth in additional detail. However, no study to date has systematically linked extracellular Ca^{2+} influx to the cytoskeleton and cell wall components in gymnosperms at the proteomic level. Such studies may be important for the integration of data at biochemical, physiological, and cellular levels.

The objective of this investigation was to explore the effects of extracellular Ca^{2+} influx on pollen tube development in *Pinus bungeana* by studying the proteomic expression profiles, the cell wall components, and the ultrastructure of pollen tubes. The results are compared to published data for angiosperms, and their relevance for tip growth is discussed.

Materials and Methods

Plant Materials and Culture Conditions. Pollen grains of *P. bungeana* were cultured in the standard media containing 0.01% H_3BO_3, 0.01% $CaCl_2$, and 15% sucrose. For inhibitors experiments, Nif was dissolved in the container to 0.01 M stock in 0.1% DMSO and then diluted to the appropriate concentrations in the standard media. Pollen cultures in flasks were incubated on a shaker (100 rpm) at 25 °C in the dark.

Pollen Tube Growth Determination and Morphological Measurements. The average pollen germination rate and pollen tube growth rate were calculated according to Hao et al.[11] The digital images of germinated tubes and the morphology of pollen tubes were captured under a Zeiss Q500 IW light microscope (Zeiss Co., Germany) with a Spot Π camera (Diagnostic Instruments, Inc.).

Measurement of Extracellular Ca^{2+} Influx. Pollens were incubated in the standard media for 72 h and then treated with 100, 250 and 500 μM Nif, respectively. Net Ca^{2+} flux was measured at Xu-Yue Sci. & Tech. Co. Ltd. (www.xuyue.net) using the noninvasive, scanning ion-selective electrode technique (SIET) as described previously.[26] The obtained data by the ion selective probe technique were analyzed by Excel spreadsheet to convert data from the background -mV estimation of concentration and microvolt difference estimation of the local gradient into specific ion influx (pmol cm^{-2} s^{-1}).

Microinjection of Calcium Green-1 Dextran. Pollen grains were fixed to a coverslip forming the bottom of a microscope slide chamber with a thin layer of media supplemented with 1% agarose (type VII; Sigma). Microinjection was performed on an Axiovert 200 M inverted microscope (Eppendorf TransferMan NK2, Germany). A total of 2.5 mM Calcium Green-1 dextran (CG-1D, 10 000 MW, Molecular Probes, Inc., Eugene, OR) in 5 mM HEPES buffer, pH 7.0, was pressure-injected into the pollen tube. The pipet tip reached no more than 3 pm into the cytoplasm of pollen tubes, and agents were gently loaded into the cytoplasm. Ca^{2+} dynamics of the injected pollen tubes was recorded using a LSM 510 META LSCM (Zeiss Co., Germany) in a time-course mode.

Protein Extraction and Two Dimensional (2D)-PAGE Analysis. Pollen tubes at different developmental stages in the control medium and media with 100 mM Nif and 200 mM Nif were collected from media, ground in liquid nitrogen and suspended in 10% (w/v) TCA in acetone with 0.07% (v/v) β-mercaptoethanol at −20 °C for 2 h with interval stirring. The samples was centrifuged at 17 000*g* for 15 min at 4 °C, then the pellets were washed twice with cold acetone containing 0.07% (v/v) β-mercaptoethanol and once with 80% acetone, followed by centrifugation for 15 min at 17 000*g*. The resulting pellets were lyophilized and then resuspended in lysis buffer, containing 7 M urea, 2 M thiourea, 2% CHAPS, 0.2% (v/v) pH 3.5−10.0 Pharmalyte, 1% DTT, 1 mM PMSF. The protein extracts were stirred for 5 min at 4 °C, water bathed for 30 min at 30 °C, and then centrifuged at 17 000*g* for 30 min at 20 °C. Protein concentration was determined by the Bradford method with a spectrophotometer (DU 640 Spectrophotometer, Beckman).

Immobilized pH gradient strips (24 cm, 3−10 L; 11 cm, 4−7 L) were rehydrated overnight with rehydrated buffer (8 M urea, 2% CHAPS, 0.5% IPG buffer, 20 mM DTT, 0.002% BRP) at 20 °C. Sample load was about 600 μg (24 cm) and 300 μg (11 cm) of protein, respectively. IFF was conducted at 20 °C in Ettan IPGphor system (GE Healthcare Life Sciences). 2D-electrophoresis was performed according to the description in Amersham Biosciences' handbook. SDS-PAGE in the second dimension was run on Ettan DALT*six* (GE Healthcare Life Sciences). For each sample analyzed, three replicas of 2-D gels were done to confirm reproducibility. Gels were stained with Coomassie brilliant blue G-250 (CBB). Image analysis was carried out with the ImageMaster 2-D Platinum version 5.0 software (GE Healthcare Life Sciences). The optimized parameters were set as saliency 2.0, partial threshold 5, and minimum area 50. All gels from each treatment were matched to each other and to the other treatments, and spots were assigned arbitrary identifiers. The quantitative comparison of the spots was based on total spot volume normalization. When the percentage of the protein volume from Nif-treated pollen tubes was up- or down-regulated by 1.5-fold compared to the control in any stage of the culture time, that is, 36 + 1, 36, 60 and 84 h, it was regarded as differentially expressed protein. The identified protein spots were manually rechecked.

Mass Spectrometry and Database Search. The digestion of proteins was carried out exactly as described previously.[10] The interested spots were manually excised from the gels and cut in about 1 mm^2 pieces. Gel slices were destained with 50 mM NH_4HCO_3 in 50% (v/v) methanol for 1 h at 40 °C. The step was repeated until the color disappeared. Gel particles were then mixed with 10 mM DTT in 100 mM NH_4HCO_3 for 1 h at 60 °C to reduce the proteins. The gels were dried in a freeze-

vacuum centrifuge for 30 min prior to incubating with 40 mM iodoacetamide in 100 mM NH_4HCO_3 for 30 min at ambient temperature in the dark to alkylate the proteins. The gel pieces were washed several times with water and completely dried in a vacuum centrifuge. Enzymatic digestion was carried out by adding gel pieces into the digestion buffer containing 100 mM NH_4HCO_3 and 5 ng/μL trypsin. The reaction mixture was kept at 37 °C for 16 h. Digested peptides were extracted by three changes of 0.1% trifluoroacetic acid (TFA) in 50% acetonitrile. The collected solutions were concentrated to 10 μL and then desalted with ZipTipC18 (Millipore, Bedford, MA). Peptides were eluted from the column with 2 μL of 0.1% TFA in 50% acetonitrile, loaded into borosilicate nanoflow tip (Micromass, U.K.), and then analyzed by electrospray ionization quadrupole time-of-flight tandem mass spectrometry (ESI-Q-TOF MS/MS, Micromass, Altrincham, U.K.). The instrument was externally calibrated using the fragmentation spectrum of the doubly charged 1571.68 Da (785.84 *m*/*z*) ion of fibrinopeptide B before loading the digested peptide samples. Protein identification was performed by searching against Mascot servers (http://www.matrixscience.com). The applied spray voltage was 800 V, with a sample cone working on 30 V. Dependent on the mass and charge state of the peptides, the collision energy was varied from 14 to 40 V. Peptide precursor ions were acquired over the *m*/*z* range 400−1900 Da in TOF-MS mode. Multiple charged (2+, 3+) ions rising above predefined threshold intensity were automatically selected for MS/MS analysis, and product ion spectra collected from *m*/*z* 50−2000. Tandem MS data were processed using the MaxEnt 3.0 (Micromass) to create peak list file. Database searches were carried out for monoisotopic peptide masses using the following parameters: A taxonomy confined to *Viridiplantae*. Trypsin was specified as the proteolytic enzyme, and one missed cleavages was allowed. Fixed modifications are not selected and variable modifications including carbamidomethylation of cysteine and oxidation of methionine are selected for searching. A peptide tolerance of ±1.2 Da for the precursor ions and a MS/MS tolerance of ±0.6 Da for the fragment ions were set. Peptide charge of +2 and +3 and monoisotopic mass was chosen, data format was set as Micromass (.PKL), and the instrument type was set to ESI-QUAD-TOF. Mascot uses a probability based on "Mowse Score" to evaluate data from MS/MS, which is reported as $-10 \times$ Log10 (p) where p is the probability that the observed match between the experimental data and the database sequence is a random event. This means that the best match is the one with the highest score. Mowse scores greater than 47 were considered significant ($p < 0.05$). The apparent p*I* and molecular weight on the original gels as well as the species investigated were also referred during protein identification.

F-Actin Staining, FM4-64 Dye Loading and Immunolabeling of Pectins. Immunofluorescence labeling of F-actin and pectins was performed according to the method described in detail by Chen et al.[27] FM4-64 loading was achieved according to Wang et al.[9] The samples were observed under LSCM with excitation at 488 nm for pectins observation and 514 nm for actin and FM4-64, respectively. Optical sections were acquired at 1 or 0.5 μM intervals in the *Z*-axis. Three dimensional reconstructions were performed with LSM 510 software (Zeiss Co., Germany).

Transmission Electron Microscopy. The control, 250 μM Nif treated pollen tubes cultured for 36 and 84 h were collected from the media. To determine the immediate effects of the inhibitor, pollen tubes were treated with Nif after they have been cultured for 36 h and then collected after treatment for only 1 h (designed as 36 + 1 h time point here). The fixation of pollen tube for electron microscopy was performed after Hao et al.[11] Sections were cut using a Leica ULTRACUT-R ultramicrotome (Leica, Germany), stained with 2% uranyl acetate (w/v) in 70% methanol (v/v) and 0.5% lead citrate, and then examined with a JEM-1230 electron microscope (JEOL Ltd., Japan).

Fourier Transform Infrared (FTIR) Microspectroscopy. Pollen tubes were collected after 84 h of incubation, washed with deionized water three times, and then frozen in vapor over liquid nitrogen immediately. After that, the samples were dried in a layer on a barium fluoride window. Spectra were obtained from the tip regions of pollen tubes with a MAGNA 750 FTIR spectrometer (Nicolet Corporation, Japan). Spectra were obtained at a resolution of 8 cm^{-1}, with 128 coadded interferograms, and normalized to obtain relative absorbance.

Results

Extracellular Ca^{2+} Flux in *P. bungeana* Pollen Tubes. Pharmacological treatment demonstrated the inhibition of germination and tube growth by Nif in a dose-dependent manner (Supplementary Figure 1). Furthermore, Nif altered normal pollen tube morphology (Supplementary Figure 2). $LaCl_3$, another Ca^{2+} commonly used channel-modulating drug, also showed dose-dependent inhibitory effects on the pollen tube development (Supplementary Figure 3). Using vibrating electrode technique, we measured Ca^{2+} influx at the extreme apex of growing pollen tubes. Ca^{2+} influx prevailed in the control tube apex and oscillated over time ($n = 5$; Figure 1). The mean maximal Ca^{2+} influx at the peak of the oscillations was 104.4 pmol cm^{-2} s^{-1} (±3.81, $n = 5$). Although the treatment with 250 and 500 μM Nif markedly decreased the magnitude of Ca^{2+} influx, it did not completely block Ca^{2+} influx at the extreme apex. The mean maximal influxes at the extreme apex after different concentrations of Nif treatment were 54.5 pmol cm^{-2} s^{-1} (±5.58, $n = 5$), 46.3 pmol cm^{-2} s^{-1} (±5.58, $n = 5$) and 33.83 pmol cm^{-2} s^{-1} (±9.65, $n = 5$), respectively, indicating that the net cytosolic Ca^{2+} concentration derived from extracellular Ca^{2+} bulk was substantially reduced in a dose-dependent manner.

Confocal Imaging of $[Ca^{2+}]_c$ Change Detected with Calcium Green-1 Dextran. The control pollen tubes showed a strong intracellular fluorescence at the tips of the pollen tubes, whereas the other regions emitted only faint fluorescence (Figure 2). Thus, a steep gradient of $[Ca^{2+}]_c$ was seen from the tip to the base. This typical tip-focused $[Ca^{2+}]_c$ appeared relatively constant during the first 60 s. After application of Nif at 75 s, the fluorescence appeared to be significantly weaker over the time in both the extreme apex and in the shank of the tube, particularly at 180 and 195 s. Finally, after approximately 195 s, the $[Ca^{2+}]_c$ gradient was completely dissipated and only weak fluorescence was observed in the extreme tip. $[Ca^{2+}]_c$ gradient dissipation was not observed in the $[Ca^{2+}]_c$ dynamics of control pollen tube as long as 195 s (Supplementary Figure 4).

Proteomic Profiles of Germinated Pollen Following Nif Treatment. Total proteins were extracted from pollen tubes after 36, 60, and 84 h treatment with two different concentrations of Nif (100 and 250 μM) to investigate the temporal characteristics of protein variation. In addition, the proteins in the pollen tubes were also extracted as early as 1 h after inhibitor application to distinguish the immediate effects of

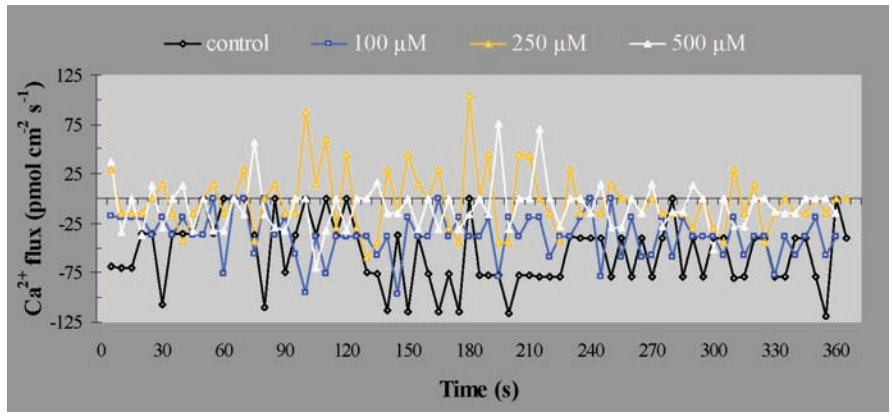

Figure 1. Dose-dependent inhibitory effects of exogenous Nif on extracellular Ca^{2+} influx at the pollen tube tips. A typical extracellular Ca^{2+} influx can be detected in the very tip of control pollen tube, and 100 μM Nif treatment decreased the Ca^{2+} influx, while 250 and 500 μM Nif treatment greatly reduced this Ca^{2+} influx.

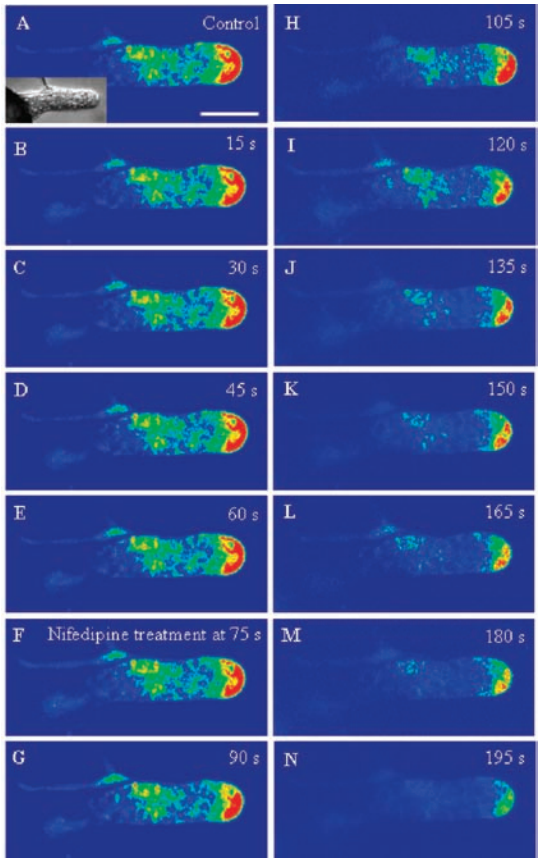

Figure 2. Time course analysis of $[Ca^{2+}]_c$ changes upon Nif treatment. Control pollen tubes exhibited a typical tip-focused $[Ca^{2+}]_c$ gradient, whereas Nif application (500 μM) rapidly decreased this $[Ca^{2+}]_c$ gradient within a couple of seconds. Finally the $[Ca^{2+}]_c$ gradient was completely dissipated and only weak fluorescence can be observed in the extreme tip after approximately 195 s. Bar =20 μM.

Nif on the pollen tube. Two-dimensional electrophoresis was performed, and approximately 700 protein spots were detected (Figure 3). Most of these proteins occurred at p*I* 4.0−7.5 with molecular weights ranging from 14 to 97 kDa. Thus, a narrow-range immobilized pH gradient (IPG; pH 4−7) was further used to prevent the spot overlap and crowding (Supplementary Figure 5). In response to Nif treatment, 50 differentially expressed proteins were identified by ESI-Q-TOF MS/MS. Because of the lack of complete genome information for conifers and the low levels of some proteins, only 34 proteins of the 50 analyzed were found to match sequences of proteins reported previously. Information about candidate proteins with high scores of confidence levels was listed in Supplementary Table 1 and Supporting Information. Of these 34 proteins, 22 were found to be highly homologous to proteins in conifers and 12 were found in other plants. Multiple spots appearing in a single gel could often be attributed to the same protein, such as spots 1 and 2, because of post-translational or chemical modification. Among the identified proteins, 15 spots showed increased expression after Nif treatment (Figure 3B), while the other 19 decreased (Figure 3B). Two proteins (spots 13 and 22) were not identified in routine searches against the National Center for Biotechnology Information databases. However, a search against the Expressed Sequence Tag (EST) database resulted in positive matches to known EST sequences. EST *viridiplantae* database searching for some proteins with only one matched peptide were performed as well (Supporting Information). This technique has been proven reliable for proteomics studies in organisms lacking sufficient genome information.[28]

The 34 identified proteins were classified into nine functional categories (Supplementary Figure 6). Because of the limitations of 2D gel-based separation and CBB staining sensitivity, the proteins were resolved in relatively higher abundance (32%, i.e., proteins related to carbohydrate and energy metabolism). The biological functions of some proteins (spots 12, 14 and 33), however, were not clearly linked to changes in the $[Ca^{2+}]_c$ gradient in pollen tube growth. In addition, two proteins (spots 15 and 34) identified in this study were difficult to classify based on the available information.

Time-Dependent Variations in Protein Expression Patterns with Varying Doses of Nif. To determine the proteins related to the primary and secondary responses to Nif, we analyzed different patterns of spot variation (Figure 4, Supplementary Figure 5 and 7). On time course analysis, 20 spots changed their intensity in a time-dependent manner. Some proteins (spots 3, 4, 6, and 21−24) showed little quantitative change in expression at 36 + 1 and 36 h after inhibitor application, while the changes were more pronounced later and maximized at 60 and 84 h. In contrast, other spots were up-regulated (spots 5 and 7−9) or down-regulated (spots 16, 17, 19, 25, 26 and 29) during the early stage of pollen tube growth with marked quantitative changes. Narrow range IPG 2D maps showed similar

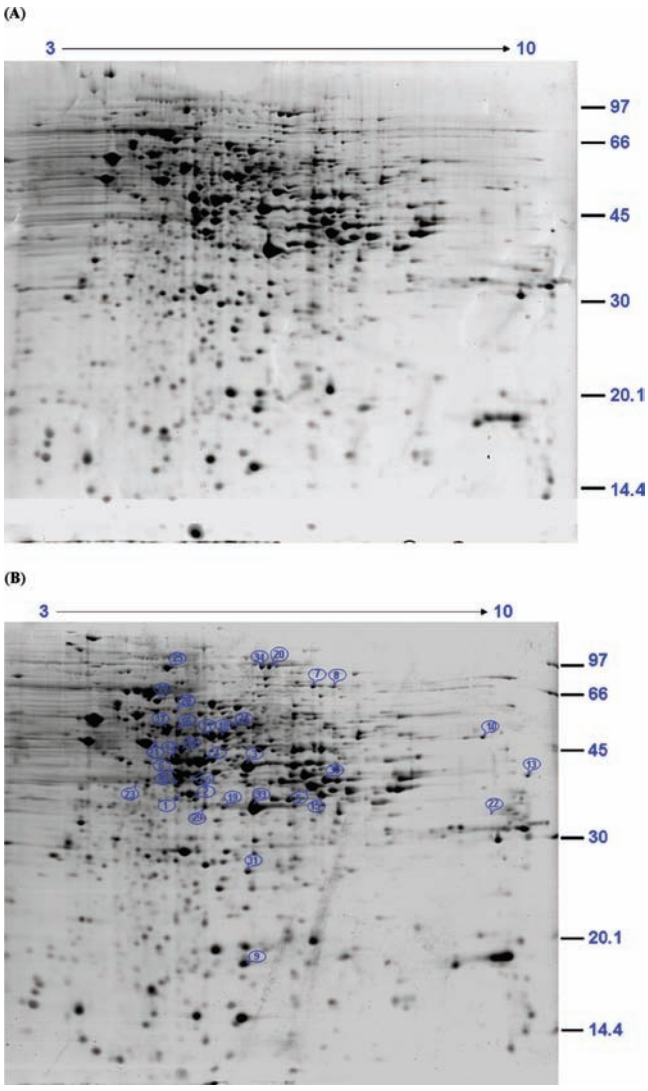

Figure 3. 2-D PAGE pattern of *P. bungeana* pollen tube proteins cultured for 84 h. The proteins were separated by first-dimensional pH 3−10 linear IPG strips and 12% vertical slab gels in the second dimension. Some selected regions are enlarged and shown in (A). Pollen tube proteins without Nif treatment (B). Fifteen up-regulated proteins (1−15) and 19 down-regulated proteins (16−34) from 250 μM Nif-treated pollen tubes.

alterations in expression of the proteins over time, further confirming the accuracy of the proteomics data (Supplementary Figure 5). We also examined the effects of Nif concentration on the protein expression in *P. bungeana* pollen subjected to 100 and 250 μM Nif for 84 h. Variation in expression level of most proteins was dose-dependent, with slight changes observed with exposure to 100 μM Nif (Supplementary Figure 7). These results demonstrated that signaling proteins (i.e., receptor protein kinase and adenosine kinase), some metabolic and energy producing proteins as primary responses, along with proteins involved in amino acid and protein synthesis and in folding and RNA binding as secondary responses were up-regulated. In contrast, some other proteins involved in metabolism, energy production, and signaling as primary responses as well as cytoskeletal proteins and proteins involved in cell wall expansion as secondary responses were down-regulated.

Nif Inhibited Pollen Tube Development and Disrupted the Actin Cytoskeleton. Inhibition of Ca^{2+} channels by Nif had profound effects on pollen tube growth, leading to disorganization of actin filaments (Figure 5). Under LSCM, the actin filaments in the control pollen tubes were organized into a contiguous network of bundles throughout the tube. These actin bundles were mainly parallel to the growth axis and excluded from the growing tip (Figure 5A,B). The organization of the actin cytoskeleton was noticeably disrupted by Nif in a dose-dependent manner. With a lower concentration of Nif in the media, the actin cytoskeleton in pollen tubes was slightly fragmented (Figure 5C). Severe disruption and fragmentation appeared in the presence of 100 and 250 μM Nif (Figure 5D,E). When the Nif concentration was increased to 500 μM, the actin cytoskeleton was completely broken into short actin filaments, which was accompanied by inhibition of pollen germination (Figure 5F).

Time Course of FM4-64 Internalization. FM4-64 uptake into the control pollen tubes showed distinct time-dependent internalization (Figure 6A−F). Fluorescence at the plasma membrane could be discerned as early as 1 min following dye application. Initial dye internalization could be seen as a slight staining of the apical cytoplasm (Figure 6B,C). This was followed by further internalization of the dye within 20 μM from the apex (Figure 6D). After 9−13 min, the typical FM4-64 staining pattern was apparent, that is, bright staining of the entire apical region in contrast to the weak staining of other regions, which corresponded to the so-called clear zone (Figure 6E,F). In Nif-treated pollen tubes, the dye internalization also began in the apical region (Figure 6G−L). However, in comparison to the control pollen tubes, FM4-64 internalization was weaker at the same time points. Furthermore, a clump-like pattern of fluorescence was distributed throughout the pollen tubes later on (Figure 6K).

Ultrastructural Changes in the Pollen Tubes in Response to Nif Treatment. Transmission electron microscopy (TEM) indicated an electron-translucent zone in the very tip of the control pollen tubes with a subapical region containing larger organelles and other cytoplasmic inclusions. We did not find specific accumulation of organelles in the extreme tip regions (Figure 7A,D,E). The cell walls of the control pollen tubes were about 0.2 μM thick at 36 h and 0.5 μM thick at 84 h, respectively (Figure 7A,D,E). Mitochondria showed intact membranes and possessed numerous well-developed cristae (Figure 8A). Golgi stacks contained 4−6 flattened cisternae with a distinct *cis*−*trans* polarity (Figure 8B). The ER was mostly flat with a large amount of ribosomes densely attached to the surfaces of the membranes (Figure 8C).

In comparison to the control pollen tube wall, Nif treatment for 1 and 36 h did not produce obvious alteration in the thickness of the tube wall (Figure 7B,C). However, some organelles emerged in the extreme apex of the tubes (Figure 7B). Furthermore, short-term Nif treatment (1 h) affected the organellar ultrastructure. Mitochondria showed slight enlargement and marked swelling of cristae (Figure 8D,G). Golgi cisternae were disintegrated and ruptured into vesicular structures (Figures 8E,H). The ER membranes became irregular, although the ribosomes were still present on the surface of ER membrane (Figure 8F,I). Thus, ultrastructural abnormalities in mitochondria and Golgi stacks occurred at early time points, therefore, representing a primary organelle-specific response induced by Nif treatment.

Long-term treatment induced pronounced ultrastructural changes (Figure 8J−L). An increasing number of vacuoles accumulated at the tips of Nif-treated pollen tubes, and a significant decrease in the thickness of pollen tube walls (0.2

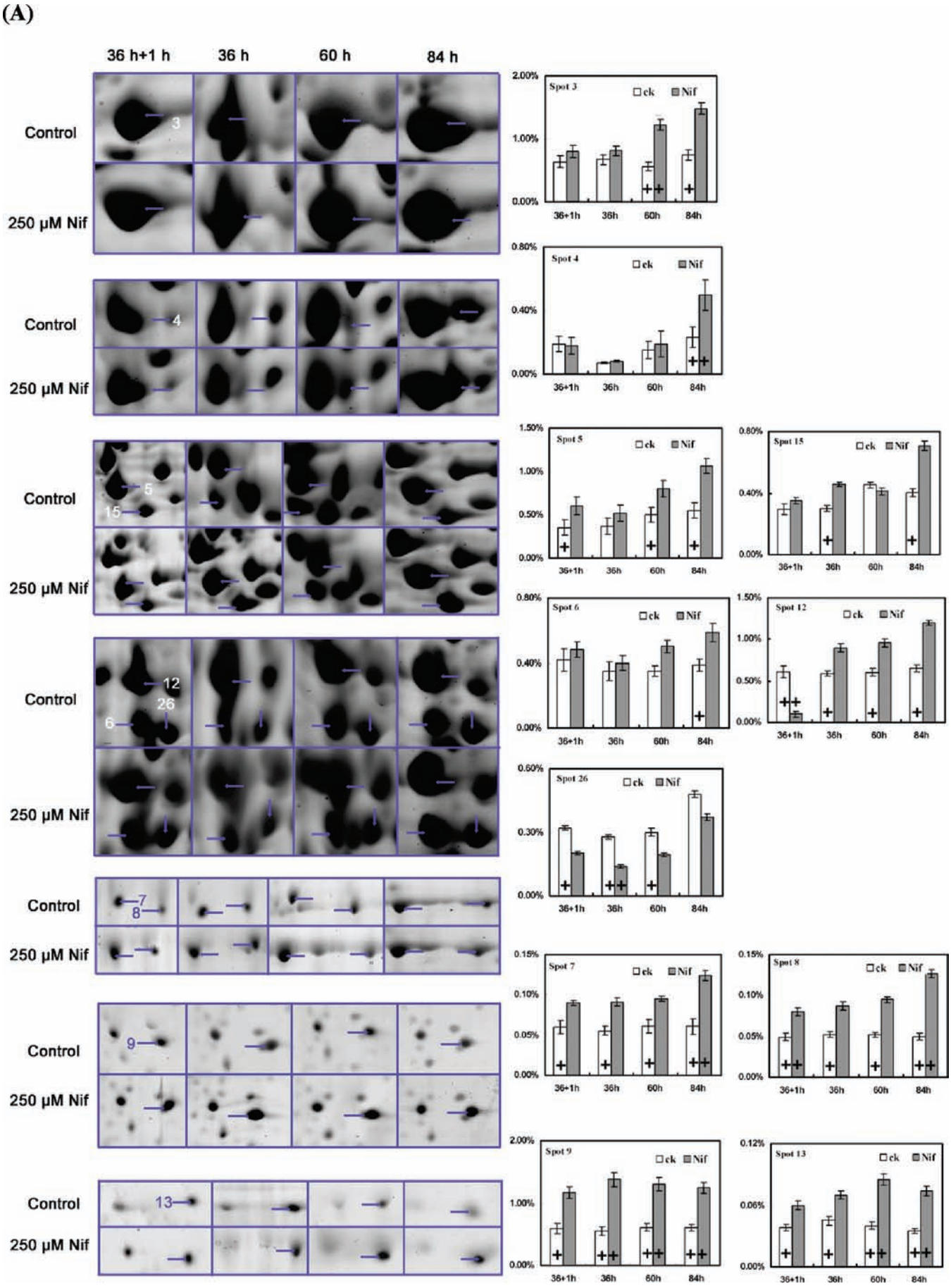

Figure 4. Continued

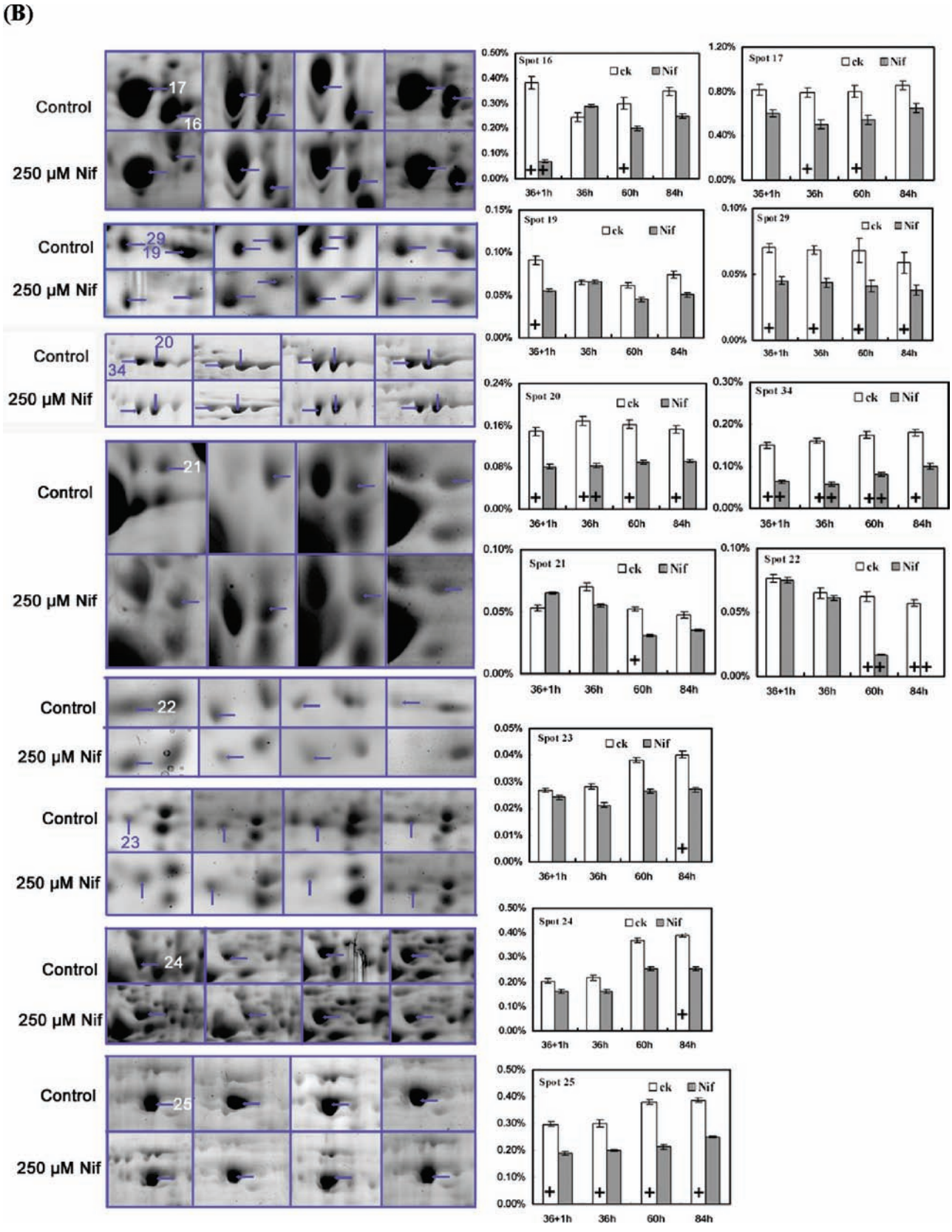

Figure 4. Variations in protein spots during pollen tube growth. Proteins were extracted from the control and Nif-treated pollen tubes cultured for 36, 60 and 84 h. To demonstrate the very short effects of Nif treatment, proteins were also extracted from the pollen tubes cultured in the standard media for 36 h and subsequently in the media with Nif for 1 h. Both up-regulated (A) and down-regulated proteins (B) showed time-dependent changes of the differentially expressed proteins. Numbered spots corresponded to Supplementary Table 1. The histograms showed the relative abundance ratio of protein (% Volume). "+" represented the change in abundance more than 1.5-fold and less than 2.0-fold after Nif treatement. "++" represented the change in abundance more than 2.0-fold after Nif treatement.

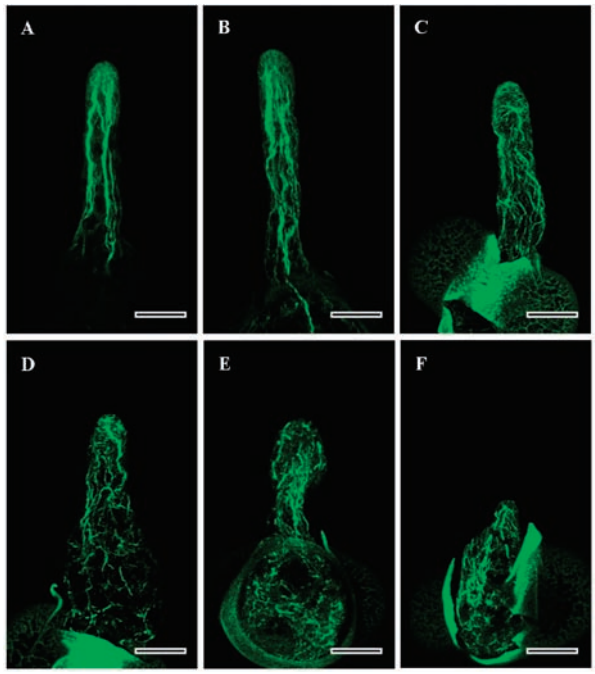

Figure 5. Nif treatment resulted in reorganization and disruption of the actin cytoskeleton in *P. bungeana* germinating pollen and pollen tubes. (A and B) The control pollen cultured for 60 and 84 h showing long pollen tubes and normal organization of actin filaments and bundles. (C) Pollen treated with 10 μM Nif for 84 h, showing slightly twisted and wavy actin cables. (D) Pollen treated with 100 μM Nif for 84 h. Inhibition of growth is accompanied by reorganization of actin cytoskeleton in the form of short and wavy actin filaments. (E) Pollen treated with 250 μM Nif for 84 h. Actin cytoskeleton is completely broken down to very short filaments and phalloidin-stained aggregates. (F) Pollen treated with 500 μM Nif for 84 h. Inhibition of pollen germination was accompanied by the severe fragmentation of actin filaments in pollen grains. Bar = 120 μM.

μM) was observed (Figure 7F,G). Mitochondria showed a reduced number of cristae and were disrupted into vacuole-like structures to various extents (Figure 8J). The Golgi apparatus tended to be fragmented, especially the *trans*-Golgi network (TGN), which ruptured into vesicle-like structures (Figure 8J−K). The ER was swollen, dilated, and fragmented, which led to the formation of irregularly shaped vesicular structures. In addition, the ribosomes appeared detached from the ER membrane (Figure 8L). These ultrastructural abnormalities in the endomembrane system may result in the breakdown of secretory pathway activities, and of the protein synthesis and modification system as secondary responses to Nif treatment. Moreover, the ultrastructural abnormalities caused by La^{3+} were also similar to that of nifedipine treatment (Supplemental Figure 8).

Changes in the Distribution/Configuration of Tube Wall Components. The JIM5 epitope was present along the cell walls and at the germinating site in pollen tubes cultured in standard media but was excluded from the tip. In the Nif-treated pollen tubes; however, the JIM5 fluorescence was distributed all over the cell walls including the apex of pollen tube, and showed a relatively homogeneous staining pattern (Figure 9A,B). The esterified pectin labeled with JIM7 was found in the walls of the tip region of control pollen tubes, in contrast to the distribution pattern of acidic pectin (Figure 9C). Esterified pectin was found in the walls of the entire tube in those showing growth suppression by 250 μM Nif (Figure 9D). Nondestructive FTIR spectroscopy confirmed immunolocalization result. The saturated ester peak at 1735 cm^{-1}, and the carbohydrate peaks between 1200 and 900 cm^{-1} were decreased, whereas the carboxylic acids bands at 1604 and 1419 cm^{-1} increased in the differential spectrum (Figure 10).

Discussion

Nif Induced Rapid Reduction of Extracelluar Ca^{2+} Influx and $[Ca^{2+}]_c$. Ca^{2+} is necessary for pollen tube elongation.[2] Although there is no doubt that the disruption of cytosolic $[Ca^{2+}]_c$ leads to cessation of pollen tube extension, the identity of the Ca^{2+} channels responsible for the extracellular Ca^{2+} influx in pollen tubes is still unclear. Franklin-Tong et al. found Ca^{2+} influx at both the apex and shank of pollen tubes could be inhibited or blocked by Ca^{2+} channel blockers, including Gd^{3+} and La^{3+}.[20] Our result of noninvasive Ca^{2+} flux detection corresponded well with the previous conclusion. However, the mean maximal Ca^{2+} influx at the peak of the *P. bungeana* pollen tubes were significantly higher than that in the angiosperm pollen tubes. Deducing from the thicker cell walls (0.5 μM in *P. bungeana* in contrast to 0.2 μM in Lily), we speculated that higher Ca^{2+} influx was necessary for gymnosperm pollen tube wall construction since incorporation of Ca^{2+} into the tube wall was necessary for pollen tube growth.[29,30] From the results of noninvasive Ca^{2+} flux detection and Calcium Green-1 dextran microinjection, we further found that the application of Nif led to a rapid reduction of extracellular Ca^{2+} influx, resulting in the dissipation of tip-focused $[Ca^{2+}]_c$. These observations indicated that the $[Ca^{2+}]_c$ gradient derives directly from influx of extracellular Ca^{2+} across the plasma membrane. Similar result was indeed reported in the previous investigations on angiosperm pollen tubes.[31] As alteration in $[Ca^{2+}]_c$ represented a rapid response to environmental stimuli and subsequently trigger downstream cytological changes, we concluded that Nif treatment induced a rapid decrease in extracellular Ca^{2+} influx as the first primary response and then gave rise to the reduce in the $[Ca^{2+}]_c$.

Nif Induced Early Alterations in Organellar Ultrastructure. A significant alteration in organellar ultrastructure occurred in most pollen tubes as early as 1 h after application of Nif; the changes included swelling and loss of cristae in mitochondria, swelling and loss of Golgi stacks, and an irregular ER structure. These events represented primary responses, which was further reinforced by TEM observations of pollen tubes after short-term treatment with La^{3+} (Supplementary Figure 8), indicating the ultrastructural changes were common responses to changes in Ca^{2+} dynamics. These substantial alterations in organellar ultrastructure were similar to those observed in the SI system of the *Papaver rhoeas* pollen tubes with respect to swelling of the mitochondria and/or rupture of their cristae, suggesting that metabolic activity may be severely affected at this early time point.[32] Nevertheless, further disruption of Golgi stacks and ER together with severe vacuolation of the mitochondria was observed after long-term treatment of Nif as secondary response to Nif.

Proteins Involved in Energy Production. A highly active metabolism is a prerequisite for pollen germination and tip growth of the pollen tube.[33,34] In our proteomic analysis, metabolic enzymes represented the most abundant category of identified proteins. Six of them were up-regulated proteins including enoyl-ACP reductase, alcohol dehydrogenase (ADH), probable mannitol dehydrogenase, and putative glutamine

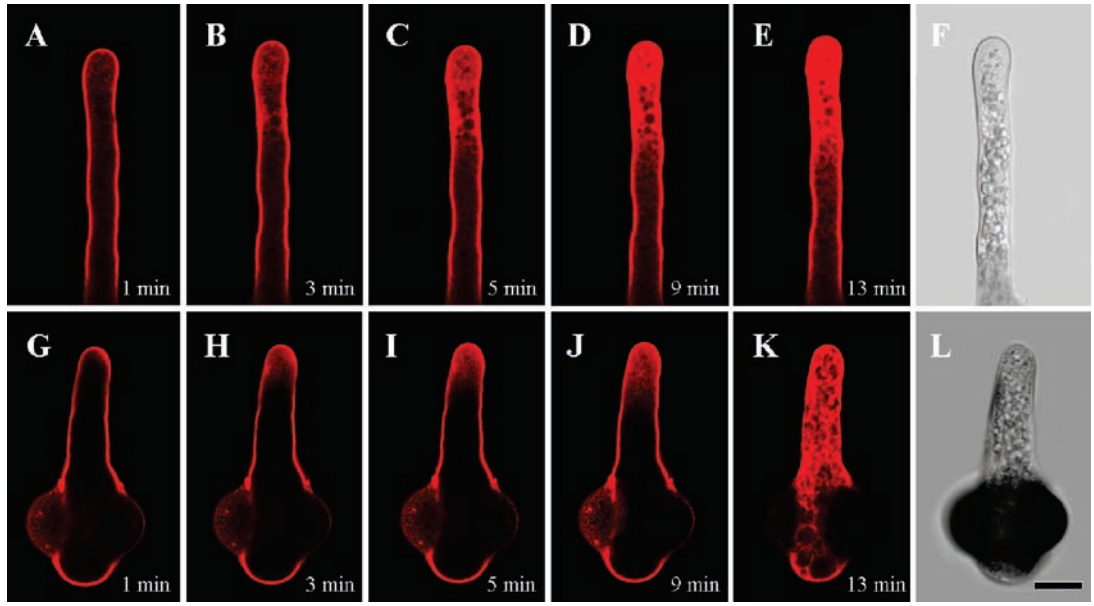

Figure 6. FM4-64-uptake time course in growing *P. bungeana* pollen tubes cultured for 84 h in standard media (A−F) and media containing 250 μM Nif (G−L). (A−E) and (G−K) Confocal fluorescence images of the control and Nif-treated pollen tubes at different times; (F and L), the corresponding bright field image. In the tip region of the control pollen tube, an extremely high rate of endocytosis and membrane traffic occurred. FM4-64 internalization process suggested Nif treatment did not inhibit the internalization of FM4-64 dye through endocytosis, but the dispersed FM4-64 distributing pattern indicated Nif inhibited transportation of secretory vesicles to the tube tip. Bar = 25 μM.

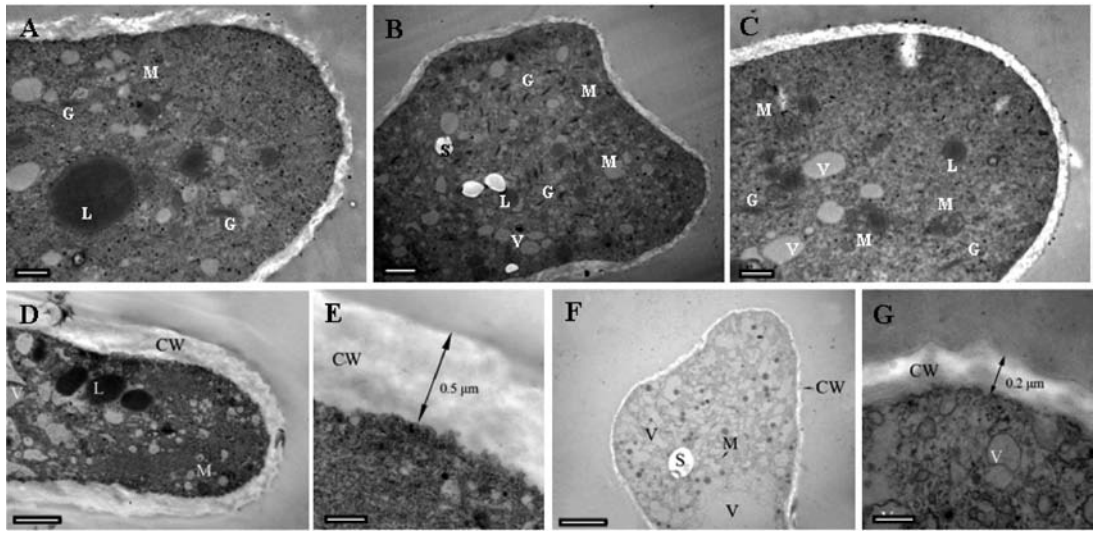

Figure 7. TEM observation of *P. bungeana* pollen tubes cultured in the standard media in the absence or presence of 250 μM Nif. (A) The control tube (36 h) showing the apical clear zone and distribution of different organelles. Bar = 1 μM. (B) The Nif-treated (1 h) pollen tube wall showing no significant alteration in thickness. Bar = 2 μM. (C) The Nif-treated (36 h) pollen tube wall showing no significant alteration in thickness. Bar = 1 μM. (D) The control pollen tube (84 h) showing the apical clear zone and distribution of different organelles. Bar = 4 μM. (E) Detail of cell wall structure in tip of control pollen tube in (D). The thickness of the cell wall was about 0.5 μM. Bar = 0.5 μM. (F) The Nif-treated (84 h) pollen tube showed accumulation of vacuoles in the swollen tip. Bar = 8 μM. (G) Details of cell wall structure in the tip of Nif-treated pollen tube in (F). The cell wall became pronouncedly thinner (0.2 μM) as compared to the control. Bar = 0.5 μM.

synthetase. Another five were down-regulated proteins, including the ATP synthase beta subunit, putative nicotinamide adenine dinucleotide (NAD) malate dehydrogenase, aconitate hydratase, and enolase. In particular, the expression of enzymes involved in the tricarboxylic acid (TCA) cycle, such as NAD-malate dehydrogenase and aconitate hydratase together with ATP synthases, decreased as early as 1 h after Nif treatment.

The up-regulation of glutamine synthetase and enoyl-ACP reductase, both of which are key regulators for the component or intermediate synthesis in TCA cycle, were significantly down-regulated in Nif-treated pollen tubes, indicating potential reduction in both the source and intermediary products involved in energy production of TCA cycle. ADH is another up-regulated protein which is abundant in tobacco pollen, but its functions in pollen remains unclear.[35] We propose that the increased expression of ADH in Nif-treated pollen tubes facilitated ethanolic fermentation to generate additional ATP, which may partly compensate for the reduction of ATP in

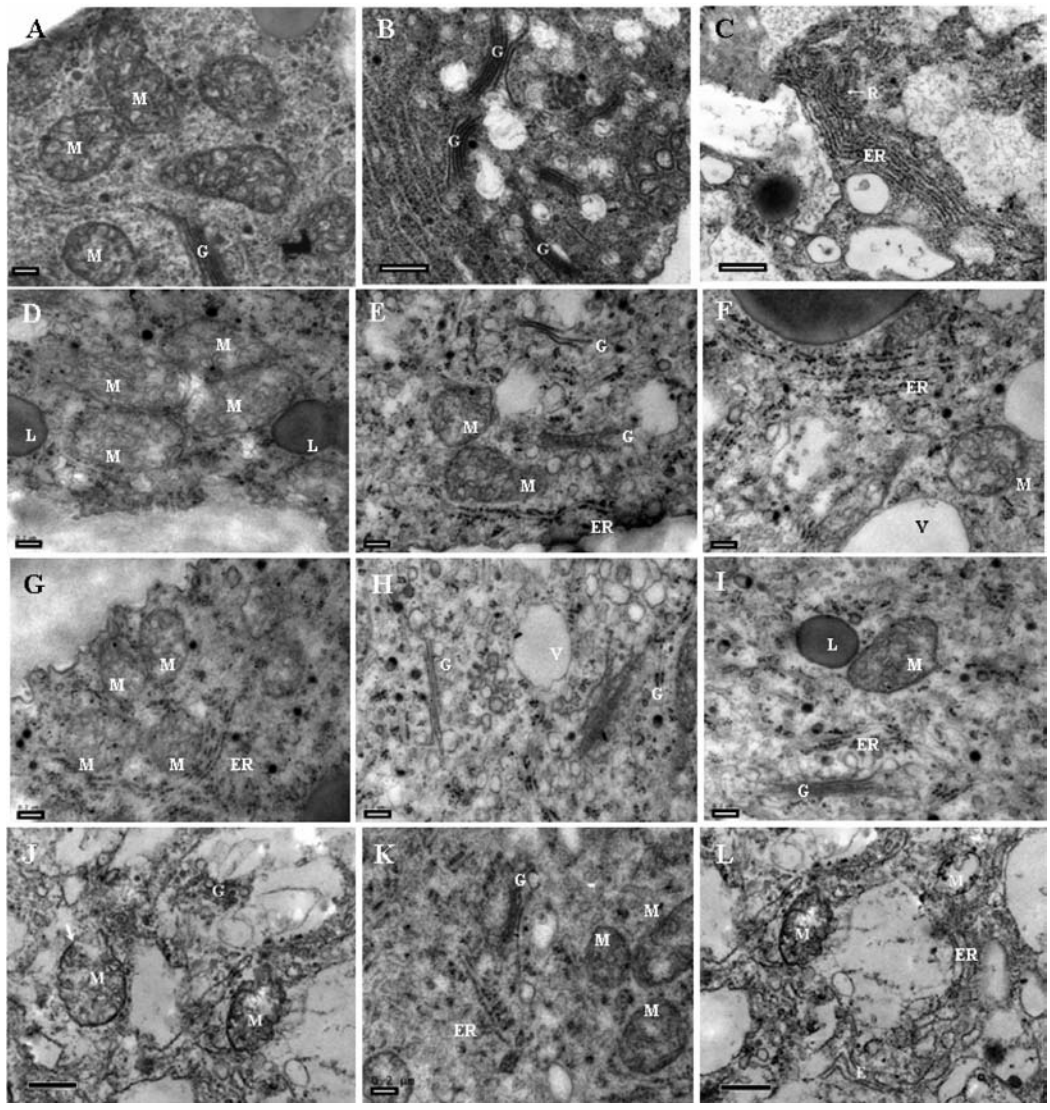

Figure 8. Organellar ultrastructure of *P. bungeana* pollen tubes cultured in the standard media in the absence or presence of 250 μM Nif. Mitochondria (A, bar = 0.5 μM), Golgi apparatus (B, bar = 0.4 μM), and endoplasmic reticulum (C, bar = 0.5 μM) in the control tube (84 h), showing normal ultrastructure; mitochondria in Nif-treated tube, showing membrane swelling and less cristae (D, 1 h; G, 36 h; bar = 0.2 μM); the fragmentation of Golgi outer cisternae in Nif-treated tube (E, 1 h; H, 36 h; bar = 0.2 μM); endoplasmic reticulum in Nif-treated tube, showing irregular membrane structure. (F, 1 h; I, 36 h; bar = 0.2 μM); mitochondria (J, bar = 0.5 μM), Golgi apparatus (K, bar = 0.2 μM), and endoplasmic reticulum (L, bar = 0.5 μM) in Nif-treated control tube (84 h), showing accelerated swelling and disrupted ultrastructure. Control (A and C) and 250 μM Nif-treated (B and D) pollen tubes cultured for 84 h were labeled with JIM 5 and JIM7, respectively, and visualized by LSCM.

glycolysis due to the production of NAD+ during conversion of acetaldehyde to ethanol by ADH, corresponding well with recent results in *Pinus strobus* using a proteomic approach.[36] Furthermore, the level of NAD-dependent mannitol dehydrogenase, which catalyzes mannitol to mannose, unexpectedly increased after treatment with Nif. We speculate that restraint of the TCA cycle may trigger alternative energy-producing bypasses to meet the enormous demand for energy and enable FM endocytic uptake into pollen tubes.[9,37]

The second group of proteins included five that were down-regulated. Enzymes involved in oxidative respiration included two mitochondrial ATP synthases, which would directly affect the generation of ATP. Enzymes in the TCA cycle, including aconitate hydratase and NAD-malate dehydrogenase, are important for the regulation of carbon flow rate in the TCA cycle. Enolase is a glycolytic enzyme that catalyzes the conversion of 2-phosphoglycerate to phosphoenol pyruvate.

High rates of synthesis and delivery of new plasma membrane precursors to the apex of the pollen tube are necessary for tip growth, which is an ATP-consuming process requiring specific carbon precursor.[33] We found that the variation in most of the proteins mentioned above reduced the metabolism intermediate in TCA and ultimately decreased the synthesis of ATP, which was also supported by evidence from TEM for mitochondria degradation at the early stage. This is consistent with evidence showing that a decline in cellular ATP associated with glucose depletion and oxidative phosphorylation results in disorganization of actin cytoskeleton.[38,39] On the basis of our results, it is reasonable to speculate that the primary effects of Nif on inhibition of ATP generation arrest of pollen tube growth. Furthermore, low $[Ca^{2+}]_c$ also triggers metabolism bypasses to compensate for the reduction in energy resulting from Nif treatment, indicating precise self-regulation in pollen tube growth.

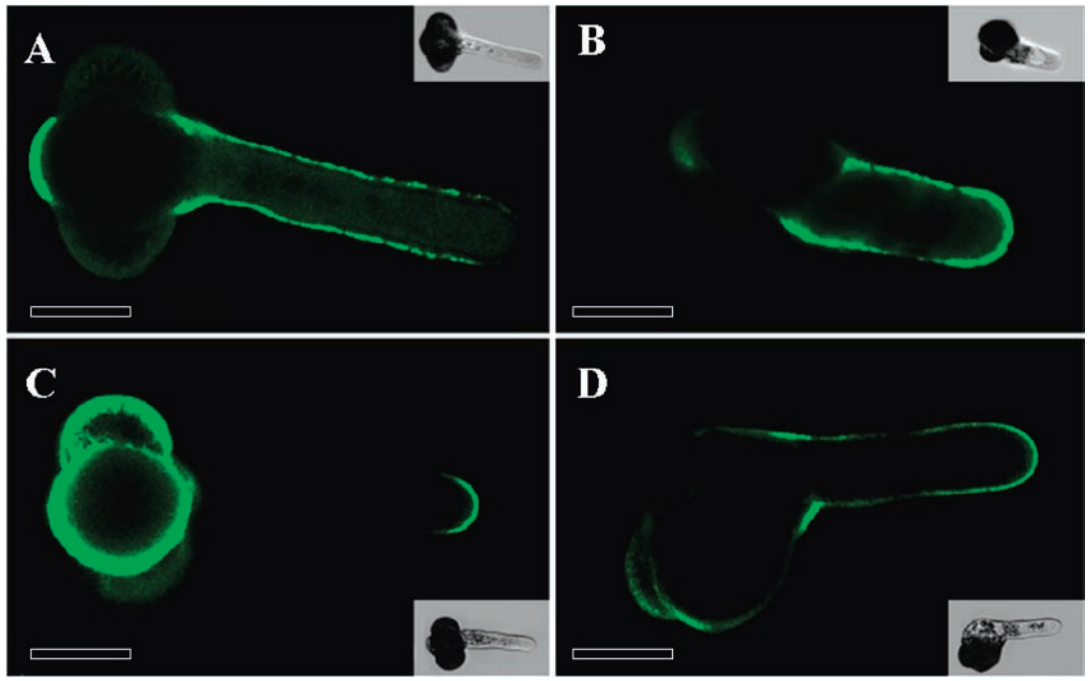

Figure 9. Effects of Nif treatment on the distribution of acidic and esterified pectin in *P. bungeana* pollen tube walls. Bar = 20 μM.

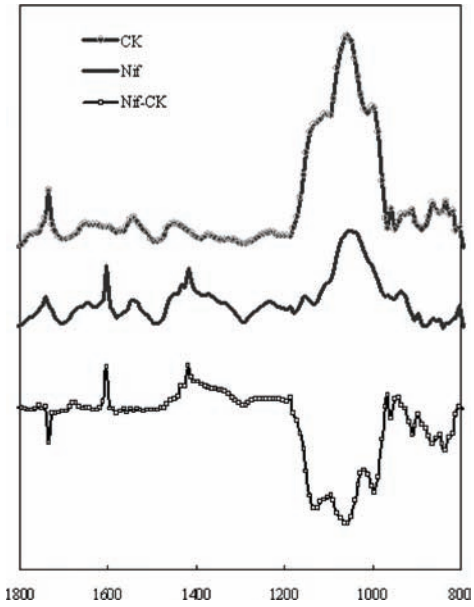

Figure 10. FTIR spectra from the tip regions of normal pollen tubes, pollen tubes treated with 250 μM Nif, and the FTIR differential spectrum generated by digital subtraction of the control spectra from the spectra of Nif-treated tube. The spectra revealed that there was less saturated ester pectin and carbohydrate, but more acid pectin present in the Nif-treated tubes.

Signaling Proteins. Of the differentially expressed spots investigated, however, only five proteins identified were involved in signal transduction: two receptor protein kinases, a valosin-containing protein (VCP) homologue, adenosine kinase and hydroxyproline-rich glycoprotein family protein. This was mainly because of the lack of complete pine genome sequence data, and the temporal and spatial features in the expression of proteins involved in signaling transduction. High levels of protein kinase activity have been detected in the growing pollen tubes of maize.[40] In *P. strobus*, protein kinase is expressed only in growing pollen tubes rather than in pollen grains.[36] The present time course analysis revealed that Nif treatment induced a rapidly increase in expression of protein receptor-like kinases (RLKs) and adenosine kinase (ADK) after 1 and 36 h treatment of Nif. Although the precise links between these RLKs and Ca^{2+} signaling remains unknown, the depression in receptor kinase could be considered a direct consequence of the blockage of L-type Ca^{2+} channel by Nif. Adenosine kinase catalyzes the salvage synthesis of adenine monophosphate from adenosine and ATP.[41] Previous investigation reported that adenosine kinase deficiency induced developmental abnormalities and reduced transmethylation.[41] By immunolocalization and biochemical techniques, Pereira et al. also revealed that deficiency of adenosine kinase activity led to the higher abundance and the altered distribution of low methyl-esterified pectin in cell walls of *Arabidopsis thaliana*.[42] Interestingly, in the present study, we also found the enhanced acid pectin in the apex pollen tube wall after Nif treatment, indicating that there is a direct correlation among Ca^{2+} influx, ADK expression and pectin methyl-esterification in pollen tubes.

VCP displaying ATPase activity may modulate protein−protein interactions in membrane transport processes of clathrin-coated pits and vesicles, which would be critical for endocytosis.[43,44] We found that decreased expression of VCP in pollen tubes of *P. bungeana* disturbed the endocytotic process, which disrupted the balance of endo/exocytosis and led to the accumulation of vesicles and vacuolation at the tips of pollen tubes. Moreover, the disruption of TGN in Nif-treated pollen tubes, as observed under TEM, further confirmed that the endocytic pathway was disturbed, which disrupted the balance of endo/exocytosis and led to the accumulation of vesicles and vacuolation at the tips of pollen tubes. Of particular importance, these results suggest that apical endocytosis in *P. bungeana* pollen tubes is regulated by the $[Ca^{2+}]_c$ gradient as reported in angiosperm pollen tubes.[45] However, there existed differences in endocytic pattern and growth rate between angiosperm and gymnosperm pollen tubes.[9,46,47] In our study, the FM4-64 staining pattern in *P. bungeana* did not demon-

strate the previously described vesicle-rich, V-shaped region as reported in angiosperm species and the cell walls in *P. bungeana* pollen tube tip were much thicker than in angiosperm.[9] On the basis of these differences, we may conclude that the slow growth rate of *P. bungeana* pollen tubes was largely attributed to the smaller region of secretory vesicles at the tip and the higher requirements of materials for tube wall construction.

Hydroxyproline-rich glycoproteins are important components of plant cell wall and play various functions, particularly serving in cell−cell interactions and communication in plant reproduction.[48] It has been reported that the pistil and pollen tube extracellular matrix are full of these highly glycosylated proteins, most of which are likely to be contributed by arabinogalactan proteins (AGPs) and extension-like proteins, regulating the pistil−pollen recognition and pollen tube growth to realize the successful fertilization.[48,49] In our study, the expression of hydroxyproline-rich glycoproteins increased over the culture time. After short-term exposure to Nif (1 and 36 h), this protein decreased in expression significantly. Therefore, it can be rationally deduced that the inhibition of pollen tube growth induced by Nif was partially attributed to the biosynthesis of cell wall components as well as wall properties.

Proteins Involved in Cytoskeleton and Cell Wall Organization. The directional transport of vesicles containing cell wall precursors is necessary for the rapid growth of pollen tubes and is dependent on the dynamics of cytoskeletal components.[50,51] In addition, the pollen tube cytoskeleton is involved in controlling cytoplasmic reorganization during tube elongation.[7] Besides, the reduced ATP production by Nif treatment would affect the ATP-dependent cytoskeleton de/polymerization and further disturb actin-dependent delivery of secretory and endocytic vesicles; two down-regulated protein spots matched the cytoskeletal proteins and would directly disarrange cytoskeletal dynamics upon Nif treatment. Alpha-tubulin is a structural unit of microtubules, along with beta-tubulin. An earlier study revealed that the stability of the microtubule cytoskeleton relies on Ca^{2+} concentration in a calmodulin-dependent manner, which is supported by the presence of short microtubules, or the complete absence of microtubules, in the apical zone.[6,52] Thion et al. demonstrated that the plasma membrane voltage-dependent Ca^{2+}-permeable channels of carrot cells could be activated by the disruption of microtubules.[53] Therefore, we postulate that reciprocal regulation of microtubules and Ca^{2+} may occur in pollen tube growth and the decreased expression of alpha-tubulin would definitely affect the assembly of microtubules, which would account for the swollen tips of pollen tubes.

The myosin-like protein, an actin-associated protein that participates in the transport of secretory vesicles by ATP-dependent sliding along actin microfilaments, was also found to be down-regulated. The decrease in its expression was accompanied by depolymerization of actin microfilaments, similar to the results reported in Nif-treated cultured rat lactotrope cells.[54] Previous studies indicated that high $[Ca^{2+}]_c$ in the extreme apex of the tube would invoke fragmentation of filamentous actin.[55] However, low $[Ca^{2+}]_c$ induced by Nif treatment in pollen tubes observed in the present study would similarly inhibit the polymerization of actin microfilaments, indicating that balanced $[Ca^{2+}]_c$ is necessary for the proper actin microfilament dynamics.

Two proteins related to cell wall formation, reversibly glycosylated polypeptide (RGP) and UDP-glucose dehydrogenase (UDPGDH), showed significant changes in their expression with long-term treatment of Nif, that is, 60 and 84 h. RGP was reported previously to be localized to the Golgi and to be involved in cell wall polysaccharide biosynthesis through reversible glycosylation.[56] The significant decrease of RGP over time indirectly supported the evident decrease in the amount of cell wall polysaccharide in the FTIR spectra. UDPGDH is a key enzyme in the biosynthesis of uronic acids, primarily D-galacturonic acid residues in the backbone of acidic pectic polysaccharides. In *Escherichia coli*, the overexpression of UDPGDH resulted in a decrease in level of glucuronic acid in the backbone of acidic pectic polysaccharides.[57] Therefore, we propose that reduced expression of UDPGDH in the Nif-treated pollen tube would increase the acidic pectin, which forms egg-carton patterns with Ca^{2+} through its carboxyl group, further leading to an increase in rigidity and a decrease in viscoelasticity of the cell wall.[32,58,59] Our immunolabeling and FTIR analysis further revealed an enhanced acidic pectin synthesis and a decrease in esterified pectin in the apex wall of Nif-treated tubes, thus, supporting our proteomic analysis. Taken together, these observations indicated that the Nif-induced decrease in expression of proteins involved in cell wall expansion and the altered composition of the cell walls led to changes in the chemical and physical properties of the cell walls, and consequently to growth inhibition.

In summary, the present study mainly focused on the proteomic and cytological variations upon the rapid decrease in the extracellular Ca^{2+} influx induced by Nif treatment. There were three major findings of the present study: (1) extracellular Ca^{2+} influx was indispensable for maintenance of the typical tip-focused $[Ca^{2+}]_c$ gradient in *P. bungeana* pollen tubes; (2) the rapid decrease of extracellular Ca^{2+} influx, subsequent reduction in $[Ca^{2+}]_c$, and dissipation of the tip-focused $[Ca^{2+}]_c$ gradient, in addition to early alterations in mitochondrial ultrastructure and changes in the abundance of signaling proteins, and proteins involved in energy production, appeared within a short time as primary responses; (3) the primary response subsequently triggered serial downstream alterations, including actin depolymerization, unbalanced endo/exocytosis, and cell wall remodeling along with the differential regulation of proteins with roles in the cytoskeleton, cell wall modeling and other functional categories, which further led to the growth arrest of *P. bungeana* pollen tubes. The combined proteomic and cytological study provided new insights into the multifaceted mechanistic framework for the functions of Ca^{2+} in the polarized tip growth of pollen tubes.

Abbreviations: CW, cell wall; ER, endoplasmic reticulum; M, mitochondrion; G, Golgi apparatus; S, starch granule; V, vacuole; L, lipid droplet.

Acknowledgment. This work was funded by the National Key Basic Research Program (2007CB108703) from MOST, the grants from NSFC (30570100 and 30700040) together with grants from Deutsche Forschungsgemeinschaft to J.Š. (DFG, SA 1564/2-1), from EU Research Training Network TIPNET (project HPRN-CT-2002-00265) obtained from Brussels, Belgium;, from Deutsches Zentrum für Luft- and Raumfahrt (DLR, Bonn, Germany); and from Grant Agency Vega (Grant No. 2031), Bratislava, Slovakia. We are sincerely grateful to Dr. Mathew Benson for his careful correction of the manuscript.

Supporting Information Available: Supplementary Table 1 shows the proteins from pollen tube proteome identi-

fied by ESI-Q-TOF MS/MS. Supporting Information 1 shows the information for protein identification by Mascot searching against NCBInr database. Supporting Information 2 shows the results for ESI *viridiplantae* database searching. Supplementary Figure 1 shows the effects of different concentrations of Nif on the pollen germination rate after cultured for 96 h. Supplementary Figure 2 shows the effects of Nif on the morphology of *P. bungeana* pollen tubes. Supplementary Figure 3 shows the effects of different concentrations of La^{3+} on the pollen germination rate after cultured for 96 h. Supplementary Figure 4 shows the time course analysis of $[Ca^{2+}]_c$ changes in the control pollen tube for a prolonged period. Supplementary Figure 5 shows the close-up of sections from 2-D gels (pH 4−7) to show the variation in the spot pattern. Supplementary Figure 6 shows the assignment of the identified proteins to functional categories. Supplementary Figure 7 shows the histograms reflecting the relative changes in amount of 34 identified proteins cultured for 84 h in different media. Supplementary Figure 8 shows organellar ultrastructures of *P. bungeana* pollen tubes cultured in the media in the absence or presence of 8 μM La^{3+}. This material is available free of charge via the Internet at http://pubs.acs.org.

References

(1) Hepler, P. K. Tip growth in pollen tubes: calcium leads the way. *Trends Plant Sci.* **1997**, *2*, 79–80.

(2) Holdaway-Clarke, T. L.; Hepler, P. K. Control of pollen tube growth: role of ion gradients and fluxes. *New Phytol.* **2003**, *159*, 539–563.

(3) Iwano, M.; Shiba, H.; Miwa, T.; Che, F. S.; Takayama, S.; Nagai, T.; Miyawaki, A.; Isogai, A. Ca^{2+} dynamics in a pollen grain and papilla cell during pollination of *Arabidopsis*. *Plant Physiol.* **2004**, *136*, 3562–3571.

(4) Schiott, M.; Romanowsky, S. M.; Baekgaard, L.; Jakobsen, M. K.; Palmgren, M. G.; Harper, J. F. A plant plasma membrane Ca2+ pump is required for normal pollen tube growth and fertilization. *Proc. Natl. Acad. Sci. U.S.A.* **2004**, *101*, 9502–9507.

(5) Yoon, G. M.; Dowd, P. E.,; Gilroy, S.; McCubbin, A. G. Calcium-dependent protein kinase isoforms in petunia have distinct functions in pollen tube growth, including regulating polarity. *Plant Cell* **2006**, *18*, 867–878.

(6) Anderhag, P.; Hepler, P. K.; Lazzaro, M. D. Microtubules and microfilaments are both responsible for pollen elongation in the conifer *Picea abies* (Norway spruce). *Protoplasma* **2000**, *214*, 141–157.

(7) Justus, C. D.; Anderhag, P.; Goins, J. L.; Lazzaro, M. D. Microtubules and microfilaments coordinate to direct a fountain streaming pattern in elongating conifer pollen tube tips. *Planta* **2004**, *219*, 103–109.

(8) Stepka, M.; Ciampolini, F.; Charzynska, M.; Cresti, M. Localization of pectins in the pollen tube wall of *Ornithogalum virens* L. Does the pattern of pectin distribution depend on the growth rate of the pollen tube? *Planta* **2000**, *210*, 630–635.

(9) Wang, Q. L.; Kong, L. A.; Hao, H. Q.; Wang, X. H.; Lin, J. X.; Šamaj, J.; Baluška, F. Effects of brefeldin A on pollen germination and tube growth: antagonistic effects on endocytosis and secretion. *Plant Physiol.* **2005**, *139*, 1692–1703.

(10) Chen, Y. M.; Chen, T.; Shen, S. H.; Zheng, M. Z.; Guo, Y. M.; Lin, J. X.; Baluška, F.; Šamaj, J. Differential display proteomic analysis of *Picea meyeri* pollen germination and pollen tube growth after inhibition of Actin polymerization by latrunculin B. *Plant J.* **2006**, *47*, 174–195.

(11) Hao, H. Q.; Li, Y. Q.; Hu, Y. X.; Lin, J. X. Inhibition of RNA and protein synthesis in pollen tube development of *Pinus bungeana* by actinomycin D and cyloheximide. *New Phytol.* **2005**, *165*, 721–730.

(12) Lazzaro, M. D.; Cardenas, L.,; Bhatt, A. P.,; Justus, C. D.; Phillips, M. S. Calcium gradients in conifer pollen tubes; dynamic properties differ from those seen in angiosperms. *JExp. Bot* **2005**, *420*, 2619–1628.

(13) Özaltin, N.; Yardimci, C.; Süslü, I. Determination of nifedipine in human plasma by square wave adsorptive stripping voltammetry. *J. Pharm. Biomed. Anal.* **2002**, *30*, 573–582.

(14) Link, Y. L.; Hofmann, M. G.; Sinha, A. K.; Ehness, R.; Strnad, M.; Roitsch, T. Biochemical evidence for the activation of distinct subsets of mitogen-activated protein kinases by voltage and defense-related stimuli. *Plant Physiol.* **2002**, *128*, 271–281.

(15) Romero, M.; Sanchez, I; Pujol, M. D. New advances in the field of calcium channel antagonists: cardiovascular effects and structure-activity relationships. *Curr. Med. Chem. Cardiovasc. Hematol. Agents* **2003**, *1*, 113–131.

(16) Roy, S. J.; Holdaway-Clarke, T. L.; Hackett, G.; Kunkel, J. G.; Lord, E. M.; Hepler, P. K. Uncoupling secretion and tip growth in lily pollen tubes: evidence for the role of calcium in exocytosis. *Plant J.* **1999**, *19*, 379–386.

(17) Shang, Z. L.; Ma, L. G.; Zhang, H. L.; He, R. R.; Wang, X. C.; Cui, S. J.; Sun, D. Y. Ca^{2+} influx into lily pollen grains through a hyperpolarization-activated Ca^{2+}-permeable channel which can be regulated by extracellular CaM. *Plant Cell Physiol.* **2005**, *46*, 598–608.

(18) Reiss, H. D.; Herth, W. Nifedipine-sensitive Ca^{2+} channels are involved in polar growth of lily pollen tubes. *J. Cell Sci.* **1985**, *76*, 247–254.

(19) Zhang, W. H.; Rengel, Z.; Kuo, J.; Yan, G. Aluminum effects on pollen germination and tube growth of *Chamelaucium uncinatum*. A comparison with other Ca^{2+} antagonists. *Ann. Bot.* **1999**, *84*, 559–564.

(20) Franklin-Tong, V. E. Involvement of extracellular calcium influx in the self-incompatibility response of *Papaver rhoeas*. *Plant J.* **2002**, *29*, 333–345.

(21) Fan, X. X.; Hou, J.; Chen, X. L.; Chaudhry, F.; Staiger, C. J.; Ren, H. Y. Identification and characterization of a Ca^{2+}-dependent actin filament-severing protein from lily pollen. *Plant Physiol.* **2004**, *136*, 3979–3989.

(22) Picton, J. M.; Steer, M. W. The effects of ruthenium red, lanthanum, fluorescein isothiocyanate and trifluoperazine on vesicle transport, vesicle fusion and tip extension in pollen tubes. *Planta* **1985**, *163*, 20–26.

(23) Šamaj, J.; Read, N. D.; Volkmann, D.; Menzel, D; Baluška, F. The endocytic network in plants. *Trends Cell Biol.* **2005**, *15*, 425–433.

(24) Salekden, G. H.; Siopongco, J.; Wade, L.; Ghareyazie, B.; Bennett, J. Proteomic analysis of rice leaves during drought stress and recovery. *Proteomics* **2002**, *2*, 1131–1145.

(25) Fernando, D. D.; Owens, J. N.; Yu, X. S.; Ekramoddoullah, A. K. M. RNA and protein synthesis during *in vitro* pollen germination and tube elongatrion in *Pinus monticola* and other conifer. *Sex. Plant Reprod.* **2001**, *13*, 259–264.

(26) Shabala, S. N.; Newman, I. A.; Morris, J. Oscillations in H^+ and Ca^{2+} ion fluxes around the elongation region of corn roots and effects of external pH. *Plant Physiol.* **1997**, *113*, 111–118.

(27) Chen, T.; Teng, N. J.; Wu, X. Q.; Wang, Y. H.; Tang, W.; Baluška, F.; Šamaj, J.; Lin, J. X. Disruption of Actin filaments by latrunculin B affects cell wall construction in *Picea meyeri* pollen tube by disturbing vesicle trafficking. *Plant Cell Physiol.* **2007**, *48*, 19–30.

(28) Kwon, K. H.; Kim, M.; Kim, J. Y.; Kim, S. I.; Park, Y. M.; Yoo, J. S. Efficiency improvement of peptide identification for an organism without complete genome sequence, using expressed sequence tag database and tandem mass spectral data. *Proteomics* **2003**, *3*, 2305–2309.

(29) Goldberg, R.; Morvan, C.; Roland, J. C. Composition, properties and localization of pectins in young and mature cells of the mung bean hypocotyl. *Plant Cell Physiol.* **1986**, *27*, 417–429.

(30) Holdaway-Clarke, T. L.; Feijo, J. A.; Hackett, G. R.; Kunkel, J. G.; Hepler, P. K. Pollen tube growth and the intracellular cytosolic calcium gradient oscillate in phase while extracellular calcium influx is delayed. *Plant Cell* **1997**, *9*, 1999–2010.

(31) Fan, L. M.; Yang, H. Y.; Zhou, C. Effects of nifedipine on pollen germination, pollen tube growth and division of generative nucleus in *Nicotiana tabacum*. *Acta Bot. Sin.* **1996**, *38*, 686–691.

(32) Geitmann, A.; Franklin-Tong, V. E.; Emons, A. C. The self-incompatibility response in *Papaver rhoeas* pollen causes early and striking alterations to organelles. *Cell Death Differ.* **2004**, *11*, 812–822.

(33) Hepler, P. K.; Vidali, L.; Cheung, A. Y. Polarized cell growth in higher plants. *Annu. Rev. Cell Dev. Biol.* **2001**, *17*, 159–187.

(34) Tadege, M.; Kuhlemeier, C. Aerobic fermentation during tobacco pollen development. *Plant Mol. Biol.* **1997**, *35*, 343–354.

(35) Tadege, M.; Dupuis, I.; Kuhlemeier, C. Ethanolic fermentation: new functions for an old pathway. *Trends Plant Sci.* **1999**, *4*, 320–325.

(36) Fernando, D. D. Characterization of pollen tube development in *Pinus strobes* (Eastern white pine) through proteomic analysis of differentially expressed proteins. *Proteomics* **2005**, *5*, 4917–4926.

(37) Gass, N.; Glagotskaia, T.; Mellema, S.; Stuurman, J.; Barone, M.; Mandel, T.; Roessner-Tunali, U.; Kuhlemeier, C. Pyruvate decarboxylase provides growing pollen tubes with a competitive advantage in Petunia. *Plant Cell* **2005**, *17*, 2355–2368.

(38) Atkinson, S. J.; Hosford, M. A.; Molitoris, B. A. Mechanism of actin polymerization in cellular ATP depletion. *J. Biol. Chem.* **2004**, *279*, 5194–5199.
(39) Pendleton, A.; Pope, B.; Weeds, A.; Koffer, S, A. Latrunculin B or ATP depletion induces profilin-dependent translocation of actin into nuclei of mast cells. *J. Biol. Chem.* **2003**, *287*, 14394–14400.
(40) Estruch, J. J.; Kadwell, S.; Merlin, E.; Crossland, L. Cloning and characterisation of a maize pollen-specific calcium-dependent calmodulin-independent protein kinase. *Proc. Natl. Acad. Sci. U.S.A.* **1994**, *91*, 8837–8841.
(41) Moffatt, B. A.; Stevens, Y. Y.; Allen, M. S.; Snider, J. D.; Pereira, L. A.; Todorova, M. I.; Summers, P. S.; Weretilnyk, E. A.; Martin-McCaffrey, L.; Wagner, C. Adenosine kinase deficiency is associated with developmental abnormalities and reduced transmethylation. *Plant Physiol.* **2002**, *128*, 812–821.
(42) Pereira, L.; Schoor, S.; Goubet, F.; Dupree, P.; Moffatt, B. Deficiency of adenosine kinase activity affects the degree of pectin methyl-esterification in cell walls of *Arabidopsis thaliana*. *Planta* **2006**, *224*, 1401–1414.
(43) Pleasure, I. T.; Black, M. M.; Keen, J. H. Valosin-containing protein, VCP, is a ubiquitous clathrin-binding protein. *Nature* **1993**, *365*, 459–462.
(44) Šamaj, J.; Baluška, F.; Voigt, B.; Schlicht, M.; Volkmann, D.; Menzel, D. Endocytosis, actin cytoskeleton, and signaling. *Plant Physiol.* **2004**, *135*, 1150–1161.
(45) Camacho, L.; Malhó, R. Endo/exocytosis in the pollen tube apex is differentially regulated by Ca^{2+} and GTPases. *J. Exp. Bot.* **2003**, *54*, 83–92.
(46) Parton, R. M.; Fischer-Parton, S.; Watahiki, M. K.; Trewavas, A. J. Dynamics of the apical vesicle accumulation and the rate of growth are related in individual pollen tubes. *J.Cell Sci.* **2001**, *114*, 2685–2695.
(47) Wang, X. H.; Teng, Y.; Wang, Q. L.; Li, X. J.; Sheng, X. Y.; Zheng, M. Z.; Šamaj, J.; Baluška, F.; Lin, J. X. Imaging of dynamic secretory vesicles in living pollen tubes of Picea meyeri using evanescent wave microscopy. *Plant Physiol.* **2006**, *141*, 1591–1603.
(48) Wu, H.; de Graaf, B.; Mariani, C.; Cheung, A. Y. Hydroxyproline-rich glycoproteins in plant reproductive tissues: structure, functions and regulation. *Cell. Mol. Life Sci.* **2001**, *58*, 1418–1429.
(49) Rubinstein, A. L.; Prata, R. T. N.; Bedinger, P. A. Developmental accumulation of hydroxyproline and hydroxyproline-containing proteins in *Zea mays* pollen. *Sex. Plant Reprod.* **1995**, *8*, 27–32.
(50) Cai, G.; Ovidi, E.; Romagnoli, S.; Vantard, M.; Cresti, M.; Tiezzi, A. Identification and characterization of plasma membrane proteins that bind to microtubules in pollen tubes and generative cells of tobacco. *Plant Cell Physiol.* **2005**, *46*, 563–578.
(51) Staiger, C. J. Signaling to the actin cytoskeleton in plants. *Annu. Rev. Plant Physiol. Plant Mol. Biol.* **2000**, *51*, 257–288.
(52) Fisher, D. D.; Gilroy, S.; Cyr, J. R. Evidence for opposing effects of calmodulin on cortical microtubules. *Plant Physiol.* **1996**, *112*, 1079–1087.
(53) Thion, L.; Mazars, C.; Thuleau, P.; Graziana, A.; Rossignol, M.; Moreau, M.; Ranjeva, R. Activation of plasma membrane voltage-dependent calcium-permeable channels by disruption of microtubules in carrot cells. *FEBS Lett.* **1996**, *393*, 13–18.
(54) Nguyen, B.; Carbajal, M. E.; Vitale, M. L. Intracellular mechanisms involved in dopamine-induced actin cytoskeleton organization and maintenance of a round phenotype in cultured rat lactotrope cells. *Endocrinology* **1999**, *140*, 3467–3477.
(55) Pierson, E. S.; Miller, D. D.; Callaham, D. A.; van Aken, J.; Hackett, G.; Hepler, P. K. Tip localized calcium entry fluctuates during pollen tube growth. *Dev. Biol.* **1996**, *174*, 160–173.
(56) Dhugga, K. S.; Tiwari, S. C.; Ray, P. M. A reversibly glycosylated polypeptide (RGP1) possibly involved in plant cell wall synthesis: purification, gene cloning, and trans-Golgi localization. *Proc. Natl. Acad. Sci. U.S.A.* **1997**, *94*, 7679–7684.
(57) Samac, D. A.; Litterer, L.; Temple, G. ; Jung, H. J.; Somers, D. A. Expression of UDP-glucose dehydrogenase reduces cell-wall polysaccharide concentration and increases xylose content in alfalfa stems. *Appl. Biochem. Biotechnol.* **2004**, *116*, 1167–1182.
(58) Franklin-Tong, V. E. Signaling and the modulation of pollen tube growth. *Plant Cell* **1999**, *11*, 727–738.
(59) Parre, E.; Geitmann, A. Pectin and the role of the physical properties of the cell wall in pollen tube growth of *Solanum chacoense*. *Planta* **2005**, *220*, 582–592.

PR800241U